Highly Responsive CO_2 Detection by an Improved & Compact Gas Sensor Using Mid-IR Spectroscopy

Mohd Rashidi Salim[1], Mohd Haniff Ibrahim[1], Asrul Izam Azmi[1], Muhammad Yusof Mohd Noor[1], Ahmad Sharmi Abdullah[1], Nor Hafizah Ngajikin[1], Hadi Manap[2], Gerard Dooly[3] and Elfed Lewis[3]
[1]*Faculty of Electrical Engineering, Universiti Teknologi Malaysia, 81310 UTM Skudai, Johor Bahru, Johor, Malaysia*
[2]*Faculty of Engineering Technology, Universiti Malaysia Pahang, 26300 Kuantan, Pahang, Malaysia*
[3]*Department of Electronic and Computer Engineering, University of Limerick, Limerick, Republic of Ireland*
rashidi@fke.utm.my

***Abstract*—An improved and compact gas sensor using mid-infrared spectroscopy for highly responsive Carbon Dioxide (CO_2) detection is presented. The sensing principle is based on open-path direct absorption spectroscopy in the mid-infrared region. The improved reflective structure of optical gas sensor consists of low cost and compact components. Several gas cell configuration which includes SISO, 2-MISO, 4-MISO and 8-MISO were simulated using ZEMAX®12 using non-sequential ray tracing technique to get the optimum radius of the reflective curved surface. Sensitivity analysis has shown that the optimised structure of 4-MISO yields the highest sensitivity and power efficiency of $-0.2895\%^{-1}$ and 12.298% respectively. The developed gas sensing system using the optimised gas cell has shown the capability of accurately detecting CO_2 concentration between 1.5% and 5.8% with no cross-sensitivity with other gases present in the gas cell. The newly developed CO_2 sensor exhibits high responsivity with the recorded rise time and fall time of less than 1 second respectively.**

***Index Terms*—Carbon Dioxide Sensor; Mid-Infrared; Responsivity; Spectroscopy.**

I. INTRODUCTION

Carbon dioxide (CO_2) has been the predominant source of pollutant gases incurred by the combustion process of fossil fuel and recognised as being one of the most influential greenhouse gases. Over the 420,000 years ago, the Earth's atmosphere which comprised of CO_2 that has periodically changed in the time frame of about 100,000 years (in conjunction with the movement of Earth's axis) from 180 to 290 parts-per-million (ppm) by volume [1]. However, the CO_2 concentration level has begun to reach the maximum value of about 280 ppm in 1850 [2]. Surprisingly, the overall level of CO_2 concentration in the Earth's atmosphere has significantly increased and reached the unprecedented level. It should be noted that the average annual concentrations of CO_2 in the atmosphere in 2013 and 2014 are 396.48 ppm and 398.55 ppm respectively. For the past decade between 2005 and 2014, the average annual increase is 2.1 ppm per year meanwhile the average for the prior decade between 1995 and 2004 is 1.9 ppm per year [3].

As illustrated in Figure 1, a large share of energy-related CO_2 emissions comes from a small number of countries. In 2012, three countries (China, United States and India) gave rise to almost half of global CO_2 emissions from fossil-fuel combustion, while ten countries (China, United States, India, Russia, Japan, Germany, Korea, Canada, Iran and Saudi Arabia) accounted for around two-thirds [4]. Since 1990, total emissions in the United States and Japan have increased slightly, while they declined by about a fifth in the European Union. After a fall of almost 30% in emissions from Russia in the early 1990s, the emissions increase after that has remained limited. In 2006, China overtook the United States as the biggest CO_2 emitter, while India overtook Russia as the fourth-largest emitter in 2009 [5].

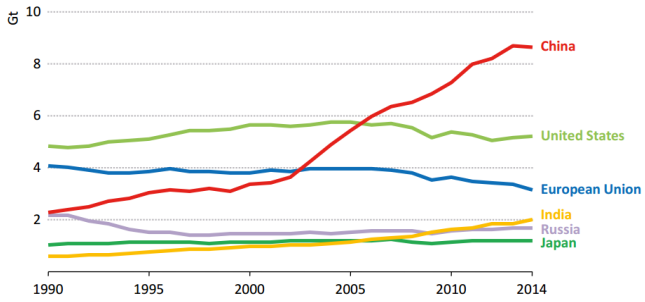

Figure 1: Energy-related CO_2 emissions from selected region [5]

Recently, there are a number of industrial processes which involved with the manufacture of CO_2 on site as the intermediate substance in producing the chemical compound. For example, a huge amount of CO_2 utilised to improve oil recuperation [6]. The use of CO_2 been extended to various types of applications by manufacturers nowadays such as in chemicals, pharmaceuticals, food and beverage, healthcare, metals industry, electronics, pulp and paper and waste treatment [7-9]. It should be noted that people with the normal function of neurological, cardiovascular, pulmonary-respiratory may not experience serious health problem underexposure of CO_2 gas concentration from 0.5% to 1.5% within the duration of up to 7 hours continuously [10]. However, longer exposure or higher concentration of CO_2 than that has significant effect on human health. It may occur if the minimum level of oxygen in the bloodstream or atmospheric air that needed to maintain people life is decreased. Besides that, people may also experience hazardous health condition if the amount of air taken during breathing is altered. For instance, human breathing rate due to physiological effects will become quicker than the effect caused by the displacement of oxygen, relying on the level of CO_2 gas concentration [10].

With thoughtful consideration to global warming issue, particularly from the standpoint of exposing to CO_2 emissions from the industrial processes, a compact and highly responsive gas sensor should be developed to monitor the presence CO_2 in the industrial environment at an early stage. Uncontrollable exposure of CO_2 to human will definitely lead to harm and could be hazardous indeed. Analyzing and designing the highly responsive and efficient CO_2 gas sensors have become subject of interest to many scholars over the last decade in order to fulfil human needs. Current existing CO_2 gas sensor normally consists of highly expensive components which constructed in bulky structure and involved complex fabrication design. Thus, a low cost and a compact CO_2 gas sensor which exhibits high responsivity should be designed properly. In this work, an improved CO_2 gas sensor for CO_2 concentration measurement using absorption spectroscopy technique is developed and analysed at low concentration. Hence, to observe the performance of the developed sensor, repeatability and responsivity of the improved sensor is compared to the previously developed sensor, particularly for measuring CO_2 at low concentration.

II. THEORY

An optical absorption based gas sensor offers fast response, very minimal drift and high gas specificity with zero cross sensitivity to others gases [11]. In terms of detection limit, lifespan, susceptibility to cross-sensitivity and ability to withstand a harsh environment, an open path absorption sensor has been proven to be the most suitable of these technologies. Sensors based on open path configuration can provide the capability of lower detection limit. An open path gas sensor is where the light is coupled into the gas cell and propagates into the free space through the measurand [12].

A. Absorption Spectroscopy

Absorption spectroscopy techniques offer direct, rapid, and often highly selective means of accurately measuring gas concentration [13]. However, to use absorption spectroscopy technique, the gas detected must have significant distinct absorption, emission or scattering in a convenient region of the optical spectrum. Different gas molecules will absorb radiation at different wavelengths, as each gas species has their own individual absorption spectrum. CO_2 has a characteristically strong absorption band in the mid-infrared region, extending from 4.2 μm to 4.5 μm, with its high peaks at 4.23 μm and 4.28 μm wavelengths as shown in Figure-2. Apart from that, CO_2 also shows a weaker corresponding near-infrared overtones absorption band around 2.7 μm, two orders of magnitude lower than that at 4.28 μm. The fundamental absorption lines of the majority of the atmospheric gases are located in the mid-infrared region with weaker overtones in the near infrared region [14]. Figure 2 illustrates the intensity of absorption by CO_2 in the mid-infrared region with the maximum CO_2 intensity of 3.543 $\times 10^{-18}$ cm^{-1} mol^{-1} cm^2.

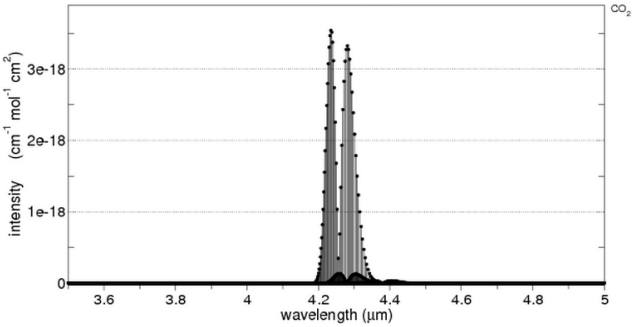

Figure 2: The absorption spectrum of CO_2 in the mid-infrared region showing its fundamental line strength at 4.23 μm and 4.28 μm [15]

B. Beer-Lambert Law

The linear relationship between absorption and concentration of an absorbing species can easily be calculated by using the Beer-Lambert law, which is shown in Equation (1). It is most commonly used to calculate how much incident radiation is absorbed by a sample. This is described in detail by many chemistry textbooks and journal [16]:

$$\ln\left(\frac{I}{I_o}\right) = -\varepsilon \times c \times l \tag{1}$$

where I is the transmitted intensity or the radiation after absorption, Io is the incident intensity or the radiation before absorption, ε (cm^2/mol) is the wavelength dependent molar absorptivity of the species, l (cm) is the optical path length, and c (mol/cm^3) is the concentration of the absorbing species.

C. Concentration Calculation

A variation of the Beer-Lambert Law was utilised by a specifically designed LabVIEW program to calculate the concentration of the gases present. The concentration of the species and a molar absorptivity of the species can also be expressed in different terms as shown as follows [12]:

$$c = \frac{c_{ppm} \times d}{w \times 10^{6}} \tag{2}$$

$$\varepsilon = \sigma \times N_A \tag{3}$$

where σ (cm^2/Molecule) is the wavelength dependent absorption cross-section of the species, w (kg/mol) is the molecular weight of the species, d (kg/cm^3) is of the density of the species in air by volume, N_A (Molecule/mol) is Avogadro's constant and c_{ppm} is CO_2 concentration in parts-per-million, or ratio of CO_2 molecules to total molecules, in the atmosphere. Hence, substituting Equation (2) and (3) into Equation (1) will give:

$$\frac{I}{I_o} = e^{-(\sigma \times N_A) \times \left[\frac{c_{ppm} \times d}{w \times 10^6}\right] \times l} \tag{4}$$

Therefore,

$$c_{ppm} = \frac{-\left[\ln \frac{I}{I_o}\right] \times w \times 10^6}{\sigma \times N_A \times d \times l} \quad (5)$$

Or,

$$\sigma = \frac{-\left[\ln \frac{I}{I_o}\right] \times w \times 10^6}{c_{ppm} \times N_A \times d \times l} \quad (6)$$

A variation of Equation (5) shown in Equation (6) is utilised to calculate the measured absorption cross section for CO_2. This measured absorption cross section represents the average of the absorption present across the full spectrum of the filter range. This value will be used during further tests to calculate the concentrations of the CO_2 present in the gas cell.

III. Proposed Approach

A reflective type of gas cell offers long path length incorporating more compact gas cell design than that of the transmissive type. It is proven from Beer-Lambert law in which absorption is directly dependent on path length of the gas cell [16]. Longer optical path length offered by the reflective gas cell than transmissive type by which indirectly raising the level of absorption by the gas species, subsequently improve the sensitivity of the system [17-18]. In the optical carbon dioxide gas sensor, the infrared radiation from optical source transmitted through the detected gas twice and doubled the optical path length, thus improve the detection accuracy [19]. In comparison, a reflective gas cell is not only compact in size but also offers better sensitivity due to its longer optical light path. The sensitivity of an open path absorption based sensor can simply be improved by increasing the path length of the gas cell. However, this will decrease the signal detected at the detector circuitry subsequently reducing the signal-to-noise ratio (SNR) of the sensor system which may affect the minimum detection limit of the sensing system. Hence, the optical path length of the gas cell should not be increased to a point where it may decrease the overall minimum detection limit of the sensing system [12].

A. Simulation

The reflective gas cell used to house the sample of gas in the optical gas sensor must be constructed from either stainless steel or aluminium due to ruggedness and relatively low cost of these metals. The optimised CO_2 sensor using single-input and single-output (SISO), 2-input and single-output (2-MISO), 4-input and single-output (4-MISO), and 8-input and single-output (8-MISO) was designed and simulated using ZEMAX®12 software to get the optimum radius of reflective curve surface using non-sequential ray tracing technique [20]. Figure 3 shows the illustration of ray tracing for SISO, 2-MISO, 4-MISO and 8-MISO of the reflective based CO_2 gas cell using a reflective curved mirror. Notice that, multiple ray colours are used in Figure 3 to show the ray propagation from one segment to another segment. As can be seen, it consists of an emitter, detector, CaF_2 window, cylinder tube, a rectangular tube and reflective curved mirror.

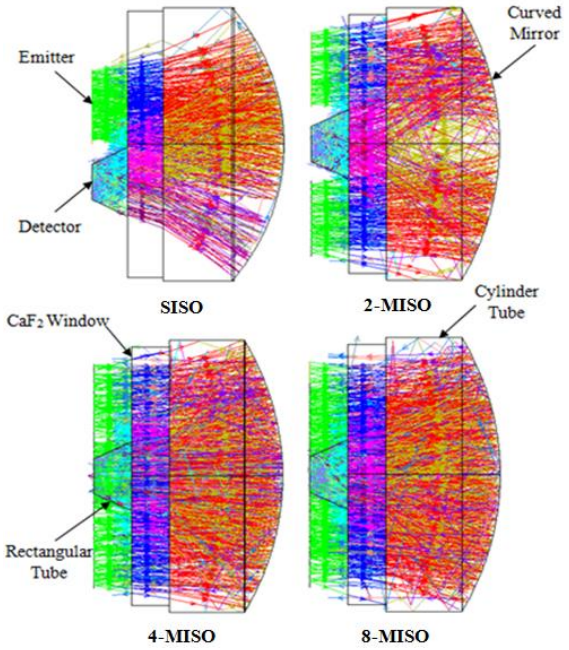

Figure 3: Ray tracing of reflective cell using single and multiple emitters; (a) SISO (b) 2-MISO (c) 4-MISO (d) 8-MISO configurations

From Table 1, SISO configuration exhibits the lowest power loss in the gas cell structure as compared to other configuration due to its maximum power efficiency of 28.03% with the lowest merit function value of 0.648. However, total power detected for SISO configuration is much less than power detected by 4-MISO and 8-MISO configurations. Regarding the level of power detection, 8-MISO configuration has the highest detected power as compared to others. However, the power efficiency of 8-MISO configuration is quite similar to 4-MISO configuration. Power efficiency can be calculated based on the following Equation (7):

$$P_{efficiency}(\%) = \frac{P_{out}}{P_{in}} \times 100\% \quad (7)$$

Table 1
Comparison of Simulated Power for Various Configuration of Gas Cell

Configuration	Optimum Radius (mm)	Supplied Input Power (mW)	Detected Output Power (mW)	Power Efficiency (%)
SISO	-30.55	1000	280.28	28.028
2-MISO	-45.38	2000	202.32	10.116
4-MISO	-42.11	4000	491.91	12.298
8-MISO	-41.54	8000	994.70	12.434

B. Sensitivity Analysis

The sensitivity of the gas sensor in this work is defined as the change in output for a given change in input, usually a unit change in input [21]. Sensitivity also refers to the sensor output per unit sensor input [22]. In this work, parameter input is the CO_2 concentration, c and parameter output is the transmittance, T_r. Clearly, sensitivity represents the slope of the graph of transmittance, T_r versus concentration, c as shown in Equation (8) [23].

$$S = \frac{T_{r1} - T_{r2}}{c_1 - c_2} \quad (8)$$

Figure 4 shows the graph of transmittance versus concentration for carbon dioxide concentration between 1.1% and 2.0%. It can be seen that the transmittance decreases as the gas concentration decreases. This is due to the drop in the detected signal power as the concentration is reduced. Since the detected reference power is constants, transmittance value is solely dependent on detected signal power. The sensitivity of the optimised gas cell configurations was calculated using Equation (8). The overall sensitivity of SISO, 2-MISO, 4-MISO and 8-MISO from 1.1% to 2% gas concentrations were calculated as being -0.2561%$^{-1}$, -0.2789%$^{-1}$, -0.2895%$^{-1}$ and -0.2681%$^{-1}$ respectively.

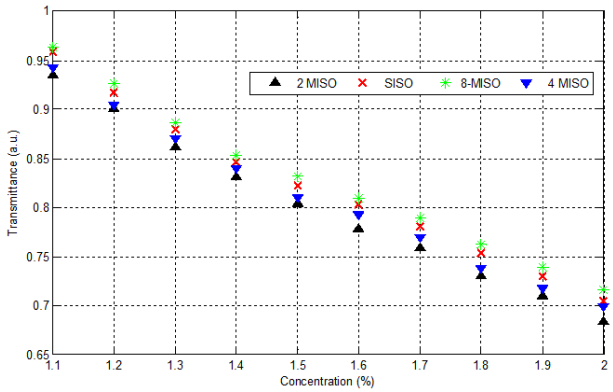

Figure 4: Graph of transmittance versus CO_2 gas concentration

Sensitivity analysis was performed on the optimised SISO, 2-MISO, 4-MISO and 8-MISO gas cell configurations based on their power detection. Simulation results have shown that SISO configuration yields the highest power efficiency of 28.03% but suffers from sensitivity issue. 4-MISO configuration yields the highest sensitivity due to its optimised structure and the positions of the optical components. The position of light sources in 4-MISO configuration has minimal scattered light effects as compared to 8-MISO configuration at which symmetrically located within a small distance to each other.

C. Optimized Gas Cell

Based on simulation results, 4-MISO configuration was selected as it exhibits the highest sensitivity and relatively good efficiency compared to other configurations with -0.2895%$^{-1}$ and 12.298% respectively. The proposed gas cell is compact as it is based on reflective type which consists of few optical components, tubes and reflective surface. Figure 5 illustrates the detailed cross-section view of the proposed reflective CO_2 gas sensor showing the light propagation and gas circulation inside the gas cell. The infrared emitters are attached on top of the gas sensor's surface subsequently reducing the transmission losses. Instead of using the highly expensive CaF_2 lens for collimating the infrared radiation as used in previous works [24-27], it is replaced with a CaF_2 window. To have better light coupling to the detector at which centred in the middle of the gas cell, the rectangular tube is attached between the CaF_2 window and the detector position. Curved surface as a reflective mirror which also made of aluminium is attached at the end of the gas cell replacing the previous flat reflective mirror used.

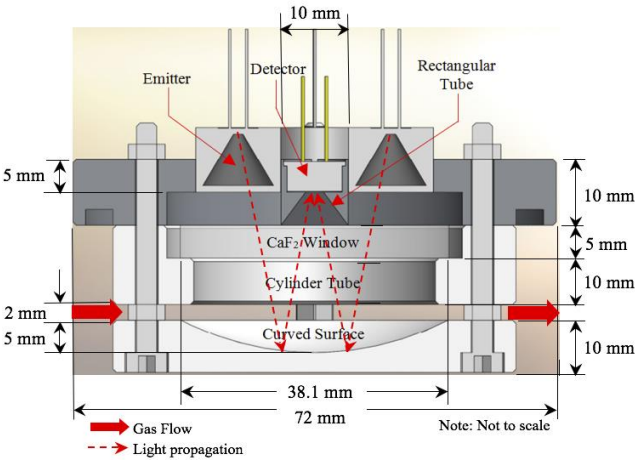

Figure 5: Cross section view of the optimised reflective CO_2 gas sensor

As depicted in Figure 5, the pulsed infrared radiation from filament emitter will be launched into the gas cell through the CaF_2 window. Following transmission into the gas chamber, the infrared radiation travelled across 10 mm of cylinder tube where it will interact with the measurand gas before coming in contact with a curved aluminium end surface. Upon contact with the curved aluminium surface, parts of the infrared radiation will be transmitted back to the same CaF_2 window where it will be confined into the rectangular tube attached to the centred pyroelectric detector.

IV. Experimental Setup

Figure 6 shows the schematic diagram of experimental set-up of the proposed reflective mid-infrared sensing system as assembled in the laboratory. The optimized gas sensor consists of low cost and compact mid-infrared region component, a broadband infrared radiation light source (2–20 μm), filament emitter reflectIR-P1C (1-10 Hz) and infrared light source evaluation kit from ion optics, LIM-262 multispectral pyroelectric detector circuitry, and also a compact reflective gas cell where curved aluminium reflective surface was used at the end of one side of the gas cell while CaF_2 window located at the other side. The window acts as a transparent barrier between the outside environment and the interior of the gas chamber. The pyroelectric detectors are fitted with two different filters, one with Narrow Bandpass filter at a centre wavelength of 4.26 μm for CO_2 detection and the other with a reference filter at a centre wavelength of 3.95 μm with a bandwidth of 180 nm and 90 nm respectively. A computer detected the voltage response of the sensor by using a National Instruments BNC 2110 Data Acquisition (DAQ) card and LabVIEW software. Both gases CO_2 and N_2 were mixed using Mass Flow Controller (MFC) to control the gas flow before purging into gas cell. The flow in and flow out of the gas before and after entering the gas cell as shown in Figure 6. A specifically designed LabVIEW program has been developed for use in the sensing system as a means of controlling data acquisition from the receiver circuitry.

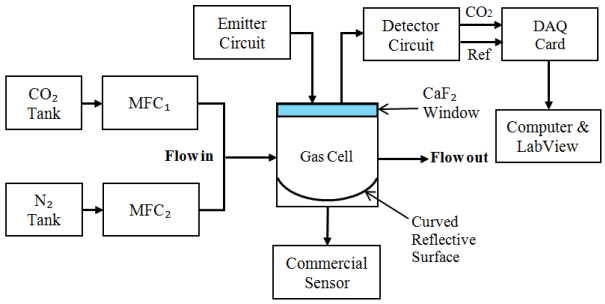

Figure 6: Schematic diagram of the experimental setup

The experimental set-up of the optimised CO_2 gas sensing system is illustrated in Figure 7. The gas flow from CO_2 and N_2 tanks were transported through the Mass Flow Controllers (MFC) to ensure more stable gas flow channelled to the optimised gas cell. The MFC used in the proposed optical sensing system is a trustworthy and well calibrated commercial gas mixer. The use of MFC has significantly affected the quality or the stability of sensor's response which described earlier. Voltage response from the sensor has shown less drift effect as reported by the previous gas sensor during initial test [24]. Besides that, the cost-effective of the proposed gas sensor has been improved as compared to the previously developed gas sensor. The proposed gas sensing system has eliminated the use of the aforementioned components. Consequently, the necessary replacement and modification are made on the structure of the gas cell to comply with the changes made.

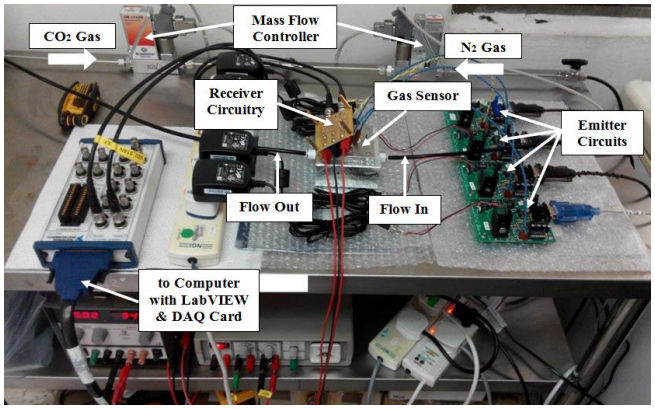

Figure 7: Experimental set-up of the CO_2 sensing system

V. Results and Discussion

Pre-measurement was carried out to determine the background intensity (due to dark current) of the multispectral pyroelectric detector, LIM-262 that used in this experiment. Background intensity, I_b is a phenomenon caused by dark spectrum and stray light. Dark spectrum is described as the intensity captured in the absence of any incident light. The measurement was completed by switching off the light source, and voltage drop was recorded for 15 minutes as shown in Figure 8. An averaged background voltage for CO_2 channel was computed to be 4.5 mV approximately. This value has to be subtracted from the recorded initial and transmitted voltage for each second to get an accurate voltage reading.

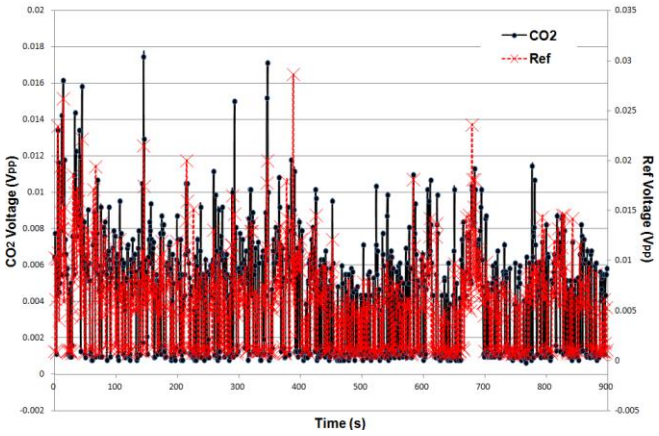

Figure 8: Background voltage, V_b response

A. *Initial Calibration*

Initial calibration was performed to estimate the measured average absorption cross section for this work. The flow rate of CO_2 and N_2 from the MFC were set to be 0.02648 ln/min and 1 ln/min respectively. As discussed in the previous paragraph, the CO_2 gas concentration of 2% would be supplied provided both of the flow rates of CO_2 and N_2 were set as calculated. Original voltage response without the presence of CO_2 is shown in Figure 9(a). Initially, N_2 gas was released at 1 ln/min to remove all the atmospheric gases which may present in the gas cell for 450 seconds. Following this, CO_2 gas was released into the gas cell at a flow rate of 0.02648 ln/min for another 450 seconds as illustrated in Figure 9(b). The commercial sensor used to validate the corresponding CO_2 concentration present inside the gas cell. Average voltage for both steps was recorded and used in Equation (6) to estimate the averaged measured absorption cross-section. The consistency of voltage response for reference as shown in Figure 9(b) proves that the developed sensor is not cross-sensitive with other gases present in the gas cell.

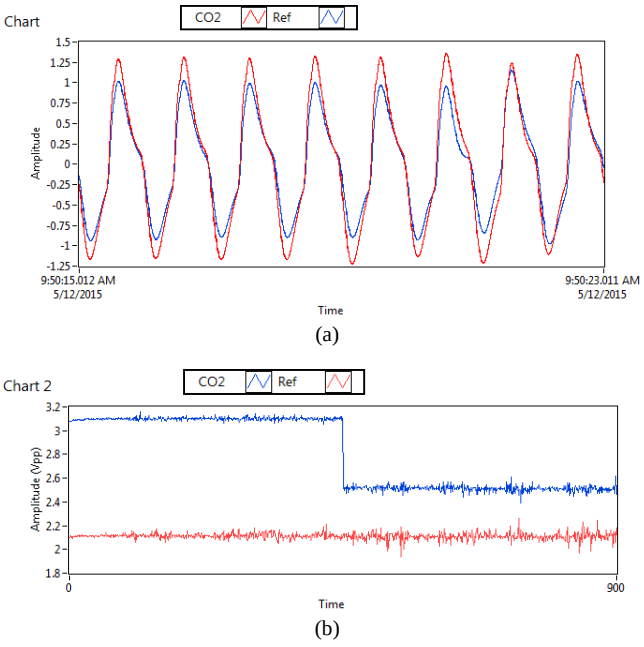

Figure 9: Measurement of averaged absorption cross section from LABVIEW (a) Original voltage response, V_{p-p} (b) Sensor voltage response

B. Concentration Measurement

The method discussed earlier was also used to calculate the respective CO_2 concentration supplied into the gas cell at various flow rates of CO_2 and N_2 gases. Figure-10 depicts the response of the sensor by varying the flow rate of N_2 at 1, 0.75, 0.5 and 0.25 ln/min while maintaining the CO_2 flow rate at 0.02648 ln/min which produced a CO_2 concentration of 1.52%, 2.01%, 2.99% and 5.81% respectively. CO_2 gas is fairly heavy gas, therefore proper and suitable flow of gas must be properly designed so that it would not take too much delay to remove the remaining CO_2 gas inside the gas cell between the concentration step transition. As discussed in earlier, the averaged absorption cross section value will be used in Equation (5) to calculate the CO_2 concentration for each step response measured by the developed CO_2 sensor throughout the measurement process. The accuracy of CO_2 gas concentration reading from the developed CO_2 sensor is then compared to the reading by the commercial sensor.

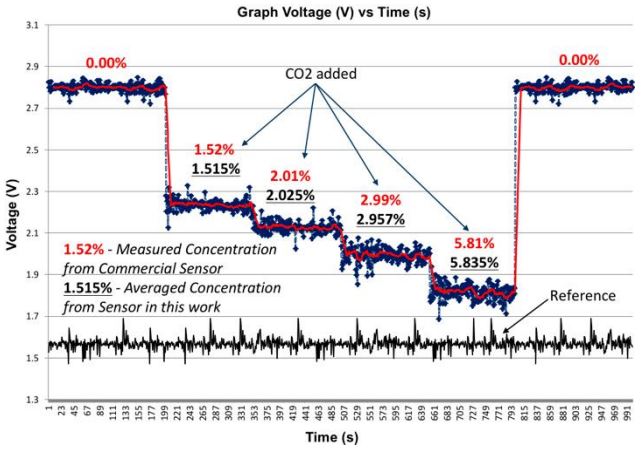

Figure 10: Graph voltage (V) vs Time (s)

Notice that, the reference output voltage remains constant throughout the measurement for 1000 seconds, indicating that there is no cross-sensitivity of the sensor to other gases present in the gas cell. Initially, the N_2 gas was purged at 1 ln/min for 200 seconds before purging CO_2 at 0.02648 ln/min and was fixed for all times. The gases were mixed for the next 200 seconds before lowering the flow rate of N_2 at 0.75 ln/min. The same process was repeated for a different flow rate of N_2 at 0.5 ln/min and 0.25 ln/min. The voltage response shows that the sensor is very responsive and has the capability of detecting the CO_2 concentration. The rise time and fall time of the sensor were calculated as being less than 1 second as shown in Figure 11 (a) and (b) respectively. This is much less than the response time recorded by the previously developed gas sensor during the initial test with a response time of 26 seconds [24]. The times are sufficient for monitoring purposes and comparable to many commercial sensors.

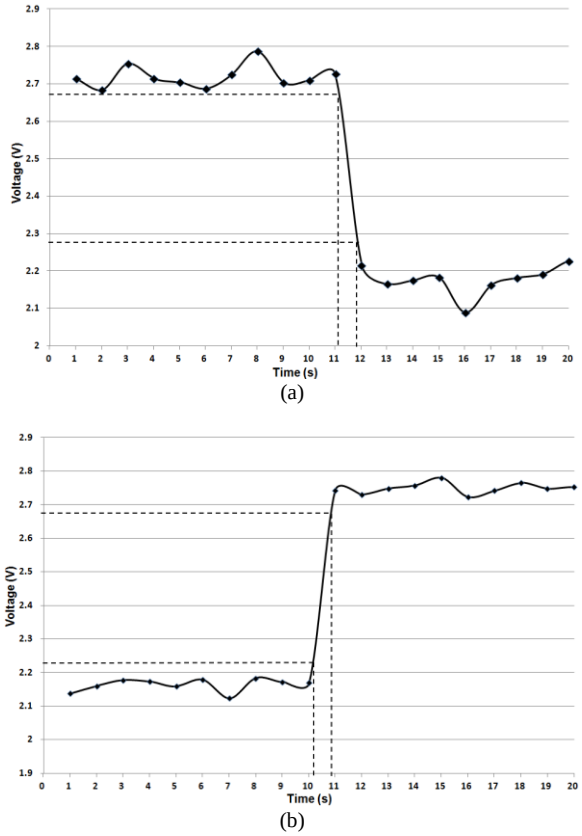

Figure 11: (a) Rise time (b) Fall time of the optimised gas sensor

VI. Conclusion

The developed sensor is compact in size, robust and constructed from inexpensive components and material. The use of the expensive lens in various sensor designs previously reported [24-27] was replaced by the optical window. The optical window which applied in reflective type for this work will absolutely need the use of curved reflective surface instead of the flat reflective surface to ensure better light coupling subsequently, reducing the transmission loss.

Few configurations of the gas cell were designed and simulated using ZEMAX®12 which include SISO, 2-MISO, 4-MISO and 8-MISO. Optimization on radius reflective surface was carried out to get the optimum radius using non-sequential ray tracing technique. Subsequently, the power detected, and the power efficiency of each configuration was analysed. Sensitivity analysis has shown that 4-MISO yields the highest sensitivity and power efficiency of $-0.2895\%^{-1}$ and 12.298% respectively. The developed CO_2 sensor is proven to be highly responsive to the calculated rise and fall time of less than 1 second respectively. The optimized sensor's reading was verified with the reading from the SenseAir commercial sensor and the measured CO_2 concentrations reading have a close agreement to that of the commercial sensor.

Acknowledgement

This work was supported by Ministry of Higher Education (MOHE), Faculty of Electrical Engineering, Research Management Centre, Universiti Teknologi Malaysia (UTM) under Potential Academic Staff Grant (Cost Center No: Q.J130000.2723.02K79).

REFERENCES

[1] Kutscher, C. (2006). Automotive Emissions and the Greenhouse Effect. July/August.

[2] Hansen, J., Johnson. D., Lacis, A., Lebedeff, S., Lee, P., Rind, D., and Russell, G. (1981). Climate Impact of Increasing Atmospheric Carbon Dioxide. Science. 213 (4511), 957-966.

[3] *How the World Passed a Carbon Threshold and Why It Matters*, Yale School of Forestry & Environmental Studies. Retrieved on August 31, 2017 from https://e360.yale.edu/features/how-the-world-passed-a-carbon-threshold-400ppm-and-why-it-matters

[4] IEA (International Energy Agency) (2013), Redrawing the Climate-Energy Map: World Energy Outlook Special Report, OECD/IEA–CO2 Emissions from Fuel Combustion 2014, OECD/IEA, Paris.

[5] *Energy and Climate Change - World Energy Outlook Special Report*. Retrieved on August 31, 2017, from https://www.iea.org/publications/freepublications/publication/WEO2015SpecialReportonEnergyandClimateChange.pdf

[6] Blunt, M., Fayers, F. J., and Orr, F. M. (1993). Carbon Dioxide in Enhanced Oil Recovery. Energy Conversion and Management. 34(9), 1197-1204.

[7] Omae, I. (2012). Recent Developments in Carbon Dioxide Utilization for the Production of Organic Chemicals. Coordination Chemistry Reviews. 256(13 14), 1384-1405.

[8] Rao, A. G., Reddy, T. S., Prakash, S. S., Vanajakshi, J., Joseph, J., and Sarma, P. N. (2007). pH Regulation of Alkaline Wastewater with Carbon Dioxide: A Case Study of Treatment of Brewery Wastewater in UASB Reactor Coupled with Absorber. Bioresource Technology. 98(11), 2131-2136.

[9] Obert, R., and Dave B. C. (1999). Enzymatic Conversion of Carbon Dioxide to Methanol: Enhanced Methanol Production in Silica Sol-Gel Matrices. Journal of the American Chemical Society. 121(51), 12192-12193.

[10] Freund, P., Bachu, S., Simbeck, D., Kelly, Thambimuthu, and Gupta, M. (2013). Properties of CO2 and Carbon-Based Fuels. IPCC Special Report on Carbon Dioxide Capture and Storage.

[11] Hodgkinson, J., Smith, R., Ho, W. O., Saffell, J. R., & Tatam, R. P. (2013). Non-dispersive infra-red (NDIR) measurement of carbon dioxide at 4.2 μm in a compact and optically efficient sensor. *Sensors and Actuators B: Chemical*, *186*, 580-588.

[12] Dooly, G. (2008). *On-Board Monitoring of Vehicle Exhaust Emissions Using an Ultraviolet Optical Fibre Based Sensor*. Doctor Philosophy. University of Limerick, Ireland.

[13] Chamber, P. (2005). *A Study of a Correlation Spectroscopy Gad Detection Method*. Doctor Philosophy, University of Southampton, U.K.

[14] Stewart, G., Jin, W., & Culshaw, B. (1997). Prospects for fibre-optic evanescent-field gas sensors using absorption in the near-infrared. *Sensors and Actuators B: Chemical*, *38*(1-3), 42-47.

[15] *Spectralcalc.com High-Resolution Spectral Modelling*. Newport News, Virginia: GATS Inc. Retrieved on April 25, 2017, from http://www.spectralcalc.com/info/about.php

[16] Peral, F., & Gallego, E. (2003). A study by ultraviolet spectroscopy on the self-association of diazines in aqueous solution. *Spectrochimica Acta Part A: Molecular and Biomolecular Spectroscopy*, *59*(6), 1223-1237.

[17] Li, M., Daia, J. M., & Pengb, G. D. (2009, July). Thin gas cell with GRIN fiber lens for intra-cavity fiber laser gas sensors. In *Proc. of SPIE Vol* (Vol. 7382, pp. 73823Q-1).

[18] Conde Portilla, O. M., García Barrio, S., Mirapeix Serrano, J. M., Echevarría Cuenca, J., Madruga Saavedra, F. J., & López Higuera, J. M. (2002, February). New optical cell design for pollutant detection. SPIE Society of Photo-Optical Instrumentation Engineers.

[19] Han, Y., Liang, T., Yang, X. J., Ren, X. L., & Yin, Y. F. (2010, September). Research on optical air chamber of infrared gas sensor. In *Pervasive Computing Signal Processing and Applications (PCSPA), 2010 First International Conference on* (pp. 33-36). IEEE.

[20] Salim, M. R., Yaacob, M., Marcus, T. C. E., David, M., Hussin, N., Ibrahim, M. H., ... & Lewis, E. (2015). Analysis of Optimized and Improved Low Cost Carbon Dioxide (CO_2) Reflective Mid-Infrared Gas Sensor. *Jurnal Teknologi (Sciences & Engineering)*, *73*(3), 63-67.

[21] Ida, N. (2014). Sensor, Actuators and their Interfaces: A Multidisciplinary Introductions. (1st eds). SciTech, Edison, NJ.

[22] Holmen, J. P. (2012). Experimental Methods for Engineers. (8th ed.). McGraw-Hill, Manhattan, 5.

[23] Marcus, T. C. E., Ibrahim, M. H., Ngajikin, N. H., and Azmi, A. I. (2015). Optical Path Length and Absorption Cross Section Optimization for High Sensitivity Ozone Concentration Measurement. Sensor and Actuators B: Chemical. 221, 570-575.

[24] Salim, M. R., Yaacob, M., Ibrahim, M. H., Azmi, A. I., Ngajikin, N. H., Dooly, G., & Lewis, E. (2015). An optical spectroscopic based reflective sensor for CO_2 measurement with signal to noise ratio improvement. *Journal of Optoelectronics and Advanced Materials*, *17*(5-6), 519-525.

[25] Dooly, G., Mulrooney, J., Merlone-Borla, E., Flavia, G., Clifford, J., Fitzpatrick, C., & Lewis, E. (2008, May). In-situ monitoring of Carbon Dioxide Emissions from a Diesel Automobile using a Mid-Infrared Optical Fibre Based Point Sensor. In *Instrumentation and Measurement Technology Conference Proceedings, 2008. IMTC 2008. IEEE* (pp. 1891-1894). IEEE.

[26] Mulrooney, J., Clifford, J., Fitzpatrick, C., & Lewis, E. (2007). Detection of carbon dioxide emissions from a diesel engine using a mid-infrared optical fibre based sensor. *Sensors and Actuators A: Physical*, *136*(1), 104-110.

[27] Muda, R., Dooly, G., Clifford, J., Mulrooney, J., Flavia, G., Merlone-Borla, E., ... & Lewis, E. (2009). Simulation and measurement of carbon dioxide exhaust emissions using an optical-fibre-based mid-infrared point sensor. *Journal of Optics A: Pure and Applied Optics*, *11*(5), 054013